A comparative study of commercial automotive prismatic Li-ion cells using nail penetration test, differential scanning calorimetry and thermogravimetric analysis

Hyojeong Kim [a,b,*], Hans Jürgen Seifert [b], Carlos Ziebert [b], Philipp Finster [b], Jochen Friedl [a]

[a] BMW Group, Battery Cell Competence Center (BCCC), Lemgostrasse 7, 80935, Munich, Germany
[b] Institute for Applied Materials – Applied Materials Physics (IAM-AWP), Karlsruhe Institute of Technology, Hermann-von-Helmholtz-Platz 1, 76344, Eggenstein-Leopoldshafen, Germany

Keywords:
Lithium-ion battery
Safety
Internal short circuit
Thermal runaway
Nail penetration
Positive electrode

A B S T R A C T

A critical penetration depth defined from a nail penetration test is an index to demonstrate, how robust a LIB cell is against internal short circuit (ISC) and thermal runaway (TR). Six different types of automotive prismatic cells are studied using nail penetration test and their resilience to the induced ISC is evaluated. Aim of this work is to comprehensively answer the question "what is(are) the key parameter(s), which define the resilience of a LIB safety against ISC on a cell level?". Several candidates as key parameter are inspected such as thicknesses of components, mass fraction of electrolyte and capacity. Among all properties, a strong correlation between safety and Ni molar fraction in NMC and NCA is found; a LIB cell consisting of cathode active material with higher Ni molar fraction tolerates less ISC and experiences TR with a smaller number of short-circuited electrodes. To understand this dependence of the safety on the cathode active material, the positive electrodes harvested from SOC 100 % LIB cells are analyzed using differential scanning calorimetry and thermogravimetric analysis. The findings suggest that the thermal stability of a positive electrode with the related electrolyte is the main factor, which determines safety on a cell level.

1. Introduction

The demand for lithium-ion batteries (LIB) has been growing with the expanding battery electric vehicle (BEV) market [1]. Since the volume and weight of LIB is directly connected to BEV's efficiency and maximum range, it is desirable to increase LIB energy density by introducing new cell dimensions and electrodes with higher gravimetric capacity. Because of thermal stability and high specific energy, NMC has become the most popular LIB's cathode material for applications, which require a high energy density. So commercial LIBs have been adopting NMC with higher Ni molar fraction, for example, from NMC111 over NMC532 and NMC622 to NMC811 [1]. Besides NMC, NCA with high nickel content became the alternative [2,3]. For example, Tesla Models S has been powered by Panasonic 18650 NCA with 3350 mAh and Model 3 is built with Panasonic 21700 NCA with 4800 mAh [4]. However, it is commonly considered that the relationship between capacity and safety is a trade-off, which means that Ni provides a high capacity but poor thermal stability [5]. Usually, Nickel-rich NMC and NCA materials show

* Corresponding author. BMW Group, Battery Cell Competence Center (BCCC), Lemgostrasse 7, 80935, Munich, Germany.
E-mail address: hyojeong.kim@bmw.de (H. Kim).

less thermal stability than alternative cathode active materials with lower nickel-content and release oxygen during decomposition reactions, which could jeopardize the safety of the batteries [1,6].That is because oxygen release damages the structure and can lead to its collapse in the layered crystal structure with a closely packed oxygen framework and interstitial metal cations [7,8].

Since the safety concern of LIB with high energy density is growing, the safety of prismatic commercial LIB cells has been evaluated under various abuse situations but most of the work has been carried out either with a limited number of LIB samples or with a wide range of samples but under different parameters. Such studies have failed to connect the behavior of thermal runaway on cell level to the thermal stability on materials level. The study conducted by Ohneseit et al. [9] employed accelerating rate calorimetry (ARC) to investigate the thermal and mechanical safety characteristics of various LIBs with different cathode materials including nickel-manganese-cobalt (NMC), nickel-cobalt-aluminum (NCA) and lithium iron phosphate (LFP) as well as varied cell designs. The findings of this study reveals that the cell chemistry can influence the overall safety of LIB cell and its susceptibility to thermal runaway. However, the study did not delve deeper into a comprehensive analysis of the cathode materials. Moreover, Doughty et al. [10] presents an investigation into the heat output during overcharge, self-heating rate and onset of self-heating from ARC with various cathode materials and DSC profiles of anode materials. Based on these results, the authors conclude that the choice of cathode material has the strongest influence on cell safety. But this study did not perform any thermal stability test of delithiated cathode material using out of cell samples. As a result, the study cannot provide conclusive evidence to the stated conclusion, even though it offers valuable insight on the correlation between the safety of LIB cell and cathode by employing a range of experimental methods. Some works have indeed tried to understand the safety of a cell by determining thermal stability of cell materials. For example, Kvasha et al. [4] studied comparatively the safety behavior of three different LIB cells with different cathode active materials using ARC, and the thermal stability of their cathode material with differential scanning calorimetry (DSC). However, the work does not replicate the same electrode-electrolyte system as it can be found in a real automotive LIB cell.

In this work, six different types of automotive prismatic LIB cells are studied using nail penetration test. The nail penetration is a widely used method to deliberately trigger internal short circuits, which is considered one of the most common causes of thermal runaway. In this work, a thin (1 mm diameter) needle was slowly inserted at a speed (1 mm/s) to induce internal shorts circuits, thereby minimizing mechanical and thermal impacts imposed on the LIB cells under abuse tests. A critical penetration depth (D_{crit}) is defined as a parameter for the ability of a cell to withstand internal short circuit (ISC) [11]. From this metric derived from the nail penetration test, the follow-up question is: what is the key-parameter for the investigated cells, which determines the critical penetration depth? The comparative study reveals that the stability of a LIB cell against ISC can be strongly affected by the thermal stability of cathode material. This assumption is followed by materials analysis of the harvested positive electrodes from each cell at 100 % state of charge (SOC). Using differential scanning calorimetry (DSC) and thermogravimetric analysis (TGA), thermal stability of cathode materials and the reaction in the positive electrode-electrolyte system have been studied. This work provides insight towards the understanding, how the safety of a LIB cell is strongly affected by the thermal stability of its positive electrode with the presence of electrolyte and serves as a guideline for future design of safer LIBs. Other parameters, which could be considered, such as capacity of the cells or thickness of the separator, are shown to have a minor influence only.

2. Experimental

2.1. Automotive prismatic LIB cell samples

The six studied types of automotive prismatic LIB cells are selected based on the following criteria:

- The cells should be commercially produced to be applied in BEV, with a high level of manufacturing precision and comparable safety features.
- The selected types should be comparable to each other, for instance, two types may be produced under comparable conditions (by the same producer), or they may exhibit comparable properties but with a specific difference to investigate the impact of that difference.

This approach ensures that the selected LIB cell types are representative of commercially available automotive cells with a high degree of quality and safety, while also allowing for a comparative analysis to elucidate the influence of specific parameters on the resilience of LIB cell against ISC.

All six types of studied automotive prismatic LIB cells have different cell dimensions, assemblies and chemistries but have similar safety elements such as vent, fuse and floating can. Cell types A and B have a dimension of 91x27 × 302 mm^3, while the cell type F has same height and depth but around half of the width (148 mm) of cell type A and B. The other three cell types C, D and E have the same dimension of 73x32x180 mm^3. The separators in the six types of LIB cells are coated with Boehmite ceramic. Whether the coating is applied on one side facing cathode or on both sides varies. While there is no distinct difference in anode active material and main electrolyte composition as determined by XRD and GC-MS, the six types of LIB cells have significantly different cathode active materials. Also, LIB cells with the same chemistry but different capacities are studied so that it is possible to understand the impact of cell capacity on thermal runaway during the abuse test. For example, cell type B and C and cell type E and F comprise the same anode, cathode and separator, but those cell types vary in size and therefore capacity. Moreover, cell type A and B with comparable capacities and cell chemistries but with different assemblies are to examine the influence of cell assembly on thermal runaway. The thickness of the electrodes is measured by metallography. Cathode and anode in all studied LIB cell types are double coated and the anode (165–220 μm) is always thicker than the cathode (120–137 μm), while the Al current collector (11–15 μm) is thicker than the Cu current collector (6–8 μm). In Table 1, the information on the six LIB cell types under investigation is listed.

2.2. Nail penetration test

The six different types of automotive prismatic LIB cells were investigated by nail penetration tests using a linear actuator manufactured by Fritz Automation GmbH to study how stable each cell is against ISC. From each cell type (A to F) two cells were analyzed and the average critical penetration depth (D_{crit}) was defined as the point, when thermal runaway is detected. The details of cell preparation and test protocol are referred to the previous work [11].

2.2.1. Cell preparation

All 12 tested LIB cell samples were fully charged to 100 % SOC by a battery tester at room temperature using a constant current (C/3) - constant voltage (break at I < 1A) protocol. Before charging, every LIB cell was compressed to 5 kN by two stainless-steel plates with a hole (diameter 15 mm) in the middle of one long side of the cell. The dimensions of the plates were chosen to entirely compress the jelly rolls or stacks within the cell.

Table 1
Information on the six studied automotive prismatic LIB cell types.

	Cell type A	Cell type B	Cell type C	Cell type D	Cell type E	Cell type F
Cell dimension	91x26.5x301.7			72.5x32 x180		91x26.5x148
Height x Depth x Width mm^3						
Capacity [Ah]	114	116	66	72	70	61
Cell assembly	Stack	Jelly rolls	Jelly rolls	Stack	Stack	Stack
Cathode active material	NMC	NMC	NMC	NMC	NCA	NCA
Anode active material	Graphite					
Separator material	PE (Boehmite coated)					
Electrolyte solvents	EC, DEC, EMC, DMC	EC, DEC, EMC, DMC	EC, DEC, EMC, DMC	EC, EMC, DMC	EC, DEC, EMC, DMC	EC, DEC, EMC, DMC
Thickness (T) [µm]						
Cell can, T_{can} (long sides)	630	507	500	500	554	553
Anode (A), T_A	180	166	165	178	220	219
Cu current collector	7	6	6	6	8	8
Separator (S), T_S	11	11	10	11	14	15
Cathode (C), T_C	137	120	120	125	134	135
Al current collector	11	14	15	13	12	12
A – S – C – S	339	308	305	325	382	384

2.2.2. Test protocol

For every test, nails made of KW 40 Carbide with a diameter of 1 mm, a length of 60 mm and a tip angle of 60° were used. The nail penetrated the center of cell with 0.01 mm/s horizontally in the direction of long side of cells, until a TR was visually observed by spark. During those nail penetration tests, the following parameters were measured; cell voltage, force applied on nail and temperatures on the surface of the cells (on vent, positive and negative terminal) using K-type thermocouples. For each cell type, the critical penetration depth (D_{crit}) that is the penetration depth, when a sudden increase in the temperature on the vent is detected, was determined for two cells.

2.3. Materials analysis

To perform thermal analysis of positive electrode materials, all six types of LIB cells were charged to SOC 100 % with the charging protocol listed in 2.2.1 and subsequently disassembled in a glove box with strict atmospheric control, both O_2 and H_2O content lower than 5 ppm.

2.3.1. Inductively coupled plasma-optical emission spectroscopy (ICP-OES)

The ICP-OES measurements were performed using the ARCOS from SPECTRO Analytical Instruments GmbH. The harvested positive electrodes were scraped with a ceramic scalpel after being rinsed with dimethyl carbonate (DMC) and being dried for 2 h at 40 °C under vacuum. 50 mg scratched cathode sample was dissolved in aqua regia (3 mL HCl and 1 mL HNO_3). The solution was held for 2 h at 90 °C and was allowed to cool and then depressurized. Following this cooling and depressurization, 5 ml of the solution, 2–3 % $Y(NO_3)_3$ concentrated in HNO_3, was added to the sample solution, then the entire sample was diluted to 50 ml with ultra-pure water prior to analysis. For the quantitative analysis of NMC and NCA, the emission lines of Li 670.780 nm, Co 237.862 nm, Mn 257.611 nm, Ni 231.604 nm and Al 396.152 nm were used.

2.3.2. Differential scanning calorimetry (DSC)

DSC 204 F1 Phoenix from Netzsch is applied to assess the thermal stability of harvested fully charged NMCs and NCAs by determining their onset temperature and the degree of reaction. The harvested positive electrode layer was not rinsed to study the positive electrode with its electrolyte. The double-side coated cathode layer including aluminum current collector was punched to a disc with 6 mm diameter and sealed tightly in a 27 µL high-pressure CrNi steel crucible with a gold-plated copper seal for two reasons; 1) to reproduce air-tight conditions in a LIB cell and 2) to prevent cathode active material from reacting with ambient air. The entire process of the sample preparation is performed in a glove box. The test was conducted from 30 to 350 °C with a 5 °C/min heating rate under argon atmosphere with weight loss under 1 %. To ensure repeatability, two tests were run for each cathode sample. The extrapolated onset temperature was determined using the software Proteus. To examine temperature reliability of this comparative DSC study, the melting point of Indium was determined as 158.9 °C with a deviation of 2.3 °C from the reference temperature of 156.6 °C, that is considered acceptable for the qualitative study. The heat release was based on the active cathode mass excluding the weight of the current collector since aluminum is thermally inactive in the studied temperature range.

2.3.3. Thermogravimetric analysis (TGA)

The TGA was carried out using STA 449 F1 Jupiter from Netzsch. The samples from the unwashed positive electrode were scraped with a ceramic scalpel. Around 10 mg of scraped positive electrodes including electrolyte and carbon black are embedded in a 27 µL stainless steel crucible with a gold-plated copper lid that has a hole in the middle. Two samples are prepared for each LIB cell and all samples are prepared in the glove box (O_2 and H_2O under 0.5 ppm). The TGA temperature profile is segmented into three parts with two 15-min isothermal phases to

divide the reaction area; 1) from 35 to 150 °C with 10 K/min where electrolyte is presumably evaporated, 2) from 150 to 300 °C with 5 K/min where it is assumed that thermal runaway would start by the exothermic cathode reactions and 3) from 300 to 500 °C with 10 K/min. The mass loss for each temperature section was evaluated using the software Proteus.

3. Results and discussion

3.1. A comparative study using nail penetration test

Since every LIB cell has various thickness of cell layers, the number of penetrated layer-sets (PLS) is defined as below.

$$\mathrm{PLS} = \frac{D_{\mathrm{crit}} - T_{\mathrm{can}}}{T_{\text{A-s-c-s}}^{*}}$$

*Thickness of double coated anode with copper current collector/separator/double coated cathode with aluminum current collector/separator.

The can thickness (T_{can}) is subtracted from the critical penetration depth (D_{crit}) under the following assumption: Every studied cell in this work has a floating can as a safety device. Therefore, it is assumed that the short circuit between cell can on positive potential and the outermost anode does not yield a significant ISC current, when those are shorted by the nail [11]. The number of penetrated layer-sets is plotted against several parameters that would have possibly a significant impact

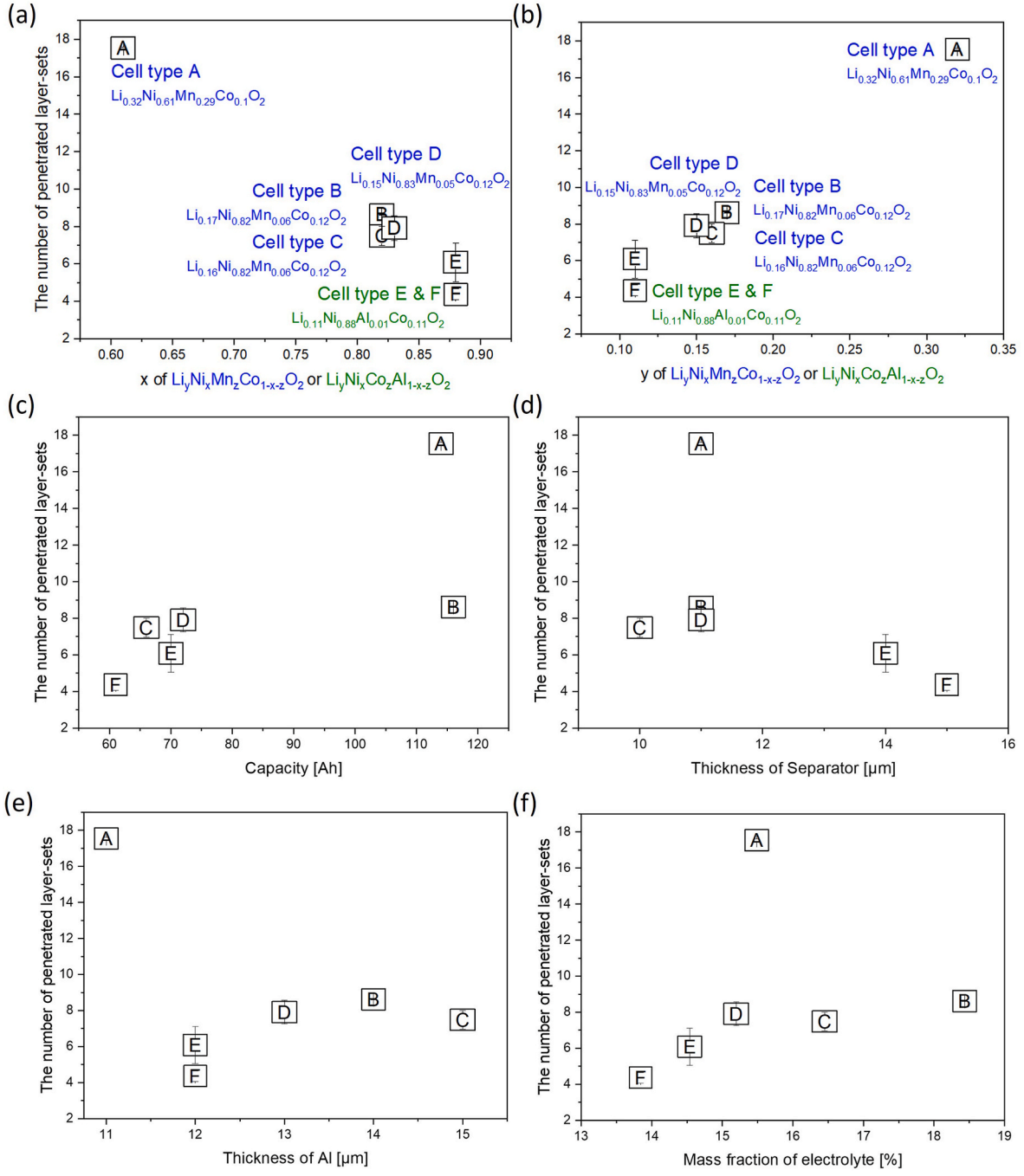

Fig. 1. The number of penetrated layer-sets and six possible influencing parameters on PLS; against Ni molar fraction(a) and Li molar fraction(b) in the cathode active material, capacity of LIB cell(c), thickness of separator(d), thickness of aluminum current collector(e) and mass fraction of electrolyte without can (f).

on PLS (see Fig. 1). These parameters are: Ni molar fraction (a) and Li molar fraction (b) in cathode active material, NMC and NCA capacity (c), thickness of separator (d), thickness of Al current collector (e) and mass fraction of electrolyte (f).

As seen in Fig. 1 a) and b), there is a correlation between PLS and the Ni molar fraction and between PLS and Li molar fraction in NMC or NCA, while there is no specific dependence found for any other parameters. For example, cell A with 114 Ah shows 17.54 PLS, while cell B with a comparable capacity of 116 Ah experiences TR with PLS of 8.62 (see Fig. 1 c)). Presumably, the capacity would have an impact on the total amount of released thermal energy from thermal runaway rather than the threshold energy to trigger thermal runaway, as Feng et al. [12] suggested the total heat generation during thermal runaway is dependent on the electrical energy of cell. Fig. 1 d) and e) present that thicker individual components, like separator and current collector, would not assure a better battery safety against internal short circuits. The separators of the six LIB cell types have various thicknesses from 10 to 15 μm. Unlike the common expectation that a thicker separator would increase the resilience of an LIB cell against ISC, cell type F with the thickest separator (15 μm) demonstrates the smallest PLS of 4.37. Also, the three cell types A, B and D with the same separator thickness of 11 μm show different PLS of 17.54, 8.62 and 7.91. There is also no trend between the thickness of the Al current collector and PLS as shown in Fig. 1 e). For example, cell type A, E and F with the comparable thickness 11 μm (A) and 12 μm (E and F) present very different resilience to ISC. Also, the mass fraction of electrolyte does not show any crucial linkage (see Fig. 1 f)). Cell type A with the highest PLS contains 15.5 wt% electrolyte, which lies in the middle of the whole range from 13.8 to 18.4 wt%. However, a possible influence of an additive in the electrolyte has been found in this work, which will be discussed in 3.2.1.

Besides the possible key parameters on PLS, some additional candidates can be taken into consideration, for instance, electrolyte solvents, cell dimensions (more specifically the area of cell layer) and cell assemblies. J.Lamb et al. [13] demonstrated that the behaviors of diethyl carbonate (DEC) and ethyl methyl carbonate (EMC) in the thermal breakdown are comparable in terms of the onset temperatures of decomposition and gas production, even though the amount of gas production varies. This supports the result that the cell type D without DEC presents the average PLS of 7.91, presenting no distinct difference from other types B and C with comparable cell chemistry. Moreover, three different cell dimensions are studied and no specific differences depending on the area of cell layer are found. Unlike above discussed possible candidates, the total number of layer sets can indeed differ depending on cell assembly: cell types (B and C) with jelly rolls have the total 48 layer-sets, while others types (A and D-F) lie in the range between 64 and 95. However, there is no correlation found between PLS and the total number of layer-sets (TLS), and in fact the ratio of PLS to TLS depends also strongly on Ni and Li molar fractions.

The Ni and Li molar fraction of the six LIB cell types is determined by ICP-OES and details are listed with the number of penetrated layer-sets in Table 2. From the weight percentage determined by the ICP-OES measurement, the chemical composition is extrapolated under the assumption that the sum of Ni, Mn (or Al) and Co molar fraction amounts to 1. As presented in Fig. 1 a) and b), a cell type with lower Li or higher Ni molar fraction tends to experience TR with smaller PLS.

An automotive prismatic LIB consists mainly of four components: cathode and anode, liquid electrolyte and separator [4]. The internally released heat of a fully charged LIB cell during nail penetration test may originate from exothermic reactions involving lithiated graphite from anode, delithiated layered metal oxide from cathode and electrolyte, respectively or in combination [14]. It can be assumed that the difference in the released heat during internal short circuit among the six different prismatic cell types would arise from the positive electrode materials, since there is no crucial difference in anode, separator and electrolyte chemistry. On top of that, Shurtz et al. [15] has shown that anode-electrolyte reactions are of modest importance in triggering thermal runaway compared to the cathode-electrolyte reactions, because the rate of heat release from the anode-electrolyte reactions is limited by the SEI layer and not sufficient to initiate thermal runaway. By high rate of heat release, the cathode reaction can be accelerated and dominates the transition to thermal runaway [16]. This theoretical statement and the fact that there is a significant difference only in cathode active materials of the samples can support the results shown in Fig. 1 a) and b) and Table 2. A LIB cell with a delithiated cathode active material that presents higher Ni molar fraction and lower Li molar fraction experiences thermal runaway with a smaller number of penetrated layer-sets, more specifically with the smaller number of individual ISC cases. As demonstrated in Table 2, it is commonly observed that a Ni-rich cathode material experiences the higher lithium extraction ratio and this leads to a significantly higher structural stress at equal LIB cell potential [17]. In addition, it is interesting to note that cell type E and F have Lithium-Nickel-Cobalt-Aluminum-Oxide (NCA), while the other cell types (Cell A to D) are with Lithium nickel manganese cobalt oxide (NMC) but both materials lie on the same trend. It is assumed that the threshold thermal energy to thermal runaway, more specifically, the battery safety against ISC is strongly dependent on the stability of the positive electrode, regardless of the composition of cathode active materials being either NMC or NCA.

3.2. *Thermal stability of NMC- and NCA based positive electrode*

In 3.1, a strong correlation is found between the stability against ISC at cell level and the Ni molar fraction (or Li molar fraction) in the studied cathode active materials, NMC and NCA. To study the materials-based thermal stability, positive electrodes are harvested from each LIB cell at SOC 100 % and investigated using DSC and TGA.

3.2.1. *DSC study*

The result from DSC with the test protocol described in 2.3.2 is presented in Fig. 2 and the average extrapolated onset temperature in Fig. 3. Many studies have investigated different cathode active materials using DSC, but most studies are limited in terms of practical validity, which means that either the studied NMCs are not extracted from a LIB cell but synthesized in laboratory (and not electrochemically but chemically delithiated) or the harvested materials are examined without electrolyte. Shurtz et al. [16] demonstrated theoretically that exothermic reactions of a delithiated cathode can be amplified in the presence of electrolyte and the generated heat per mole of delithiated

Table 2
Chemical composition of the six LIB cell types and their related number of penetrated layer-sets.

Cell	ICP [wt.%]					Cathode active material	PLS		
	Li	Ni	Mn/Al	Co	O		1	2	Average
A	2.40	38.8	17.64	6.29	34.84	$Li_{0.32}Ni_{0.61}Mn_{0.29}Co_{0.1}O_2$	17.58	17.49	17.54
B	1.31	52.55	3.59	7.68	34.73	$Li_{0.17}Ni_{0.82}Mn_{0.06}Co_{0.12}O_2$	8.64	8.60	8.62
C	1.20	52.04	3.62	7.58	34.59	$Li_{0.16}Ni_{0.82}Mn_{0.06}Co_{0.12}O_2$	7.12	7.85	7.49
D	1.07	51.61	2.67	7.57	33.80	$Li_{0.15}Ni_{0.83}Mn_{0.05}Co_{0.12}O_2$	8.37	7.45	7.91
E	0.94	62.45	0.41	7.76	38.74	$Li_{0.11}Ni_{0.88}Al_{0.01}Co_{0.11}O_2$	6.82	5.36	6.09
F	0.93	62.40	0.43	7.77	38.75	$Li_{0.11}Ni_{0.88}Al_{0.01}Co_{0.11}O_2$	4.58	4.16	4.37

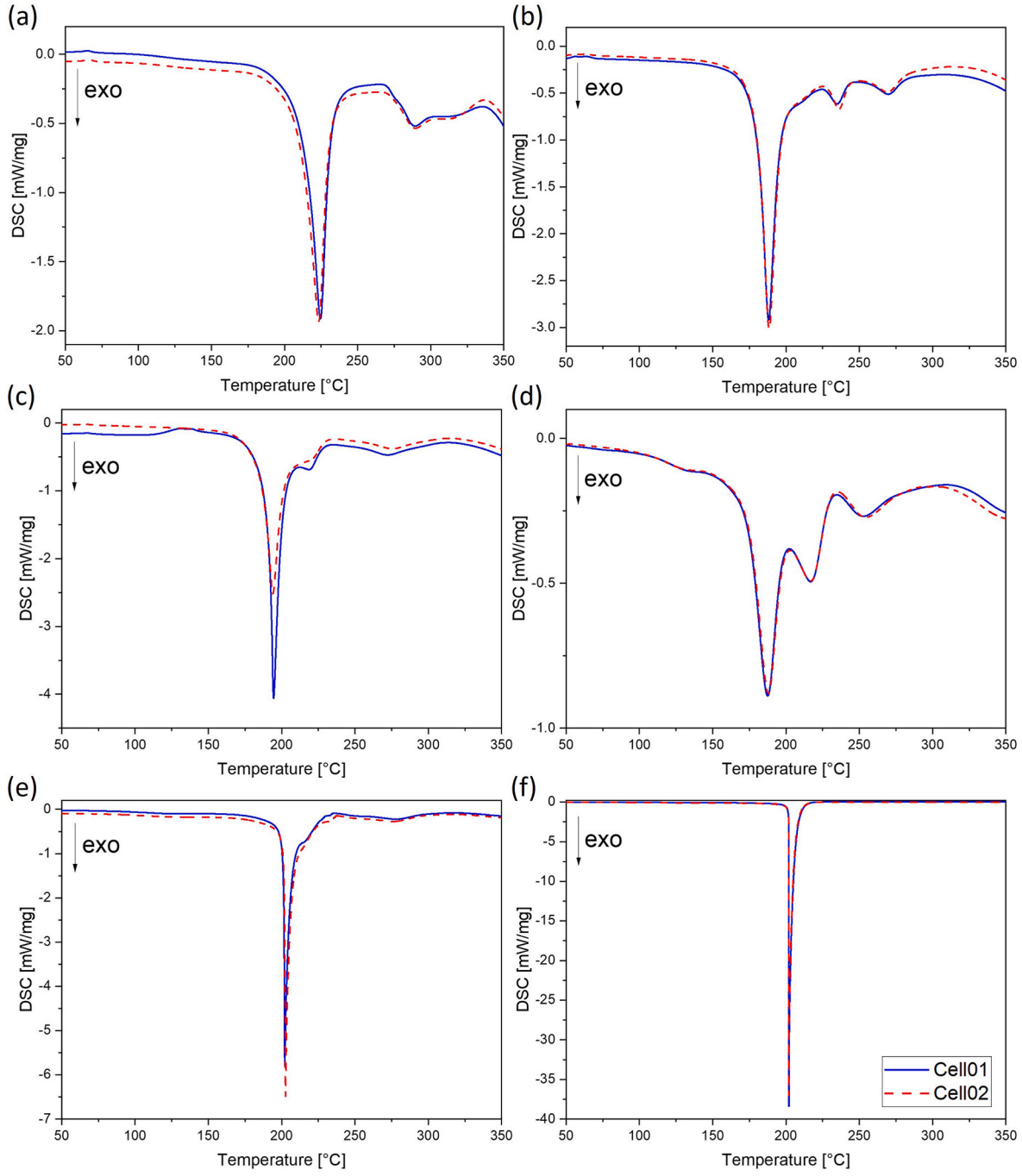

Fig. 2. DSC studies with the harvested positive electrode from 100 % SOC LIB cells: (a) Cell type A, (b) Cell type B, (c) Cell type C, (d) Cell type D, (e), Cell type E and (f) Cell type F. Each cell was studied twice, and each is presented with single blue line and dashed red line. (For interpretation of the references to colour in this figure legend, the reader is referred to the Web version of this article.)

metal oxide can be increased by 10 % in the presence of electrolyte. As electrolyte will always be present in a working LIB cell, it is therefore plausible that a DSC study should be conducted with electrolyte. To preserve the condition of cathode DSC investigation and cathode environment in a LIB cell as similar as possible, the extracted positive electrode layer including Al current collector, carbon black and electrolyte was embedded in an air-tight crucible without time delay (less than an hour).

All samples experience exothermic reactions in the temperature range from around 170 to 250 °C. Presumably, the generated heat would originate from the decomposition of NMC or NCA and the oxidation reaction of the electrolyte. The extrapolated onset temperature seen in Fig. 3 is only comparatively studied between LIB cells based on the temperature reliability test by the measurement of Indium's melting point as described in 2.3.2.

The following can be observed and extracted from Figs. 2 and 3:

a. The two measurements from each LIB cell yield very similar results in Fig. 2.
b. Cell type A presenting the highest onset temperature 211 °C, i.e., with a thermally more stable NMC cathode, experiences thermal runaway with the highest PLS (17.54) compared to cell types B, C and D with lower onset temperatures from 173 to 188 °C. This

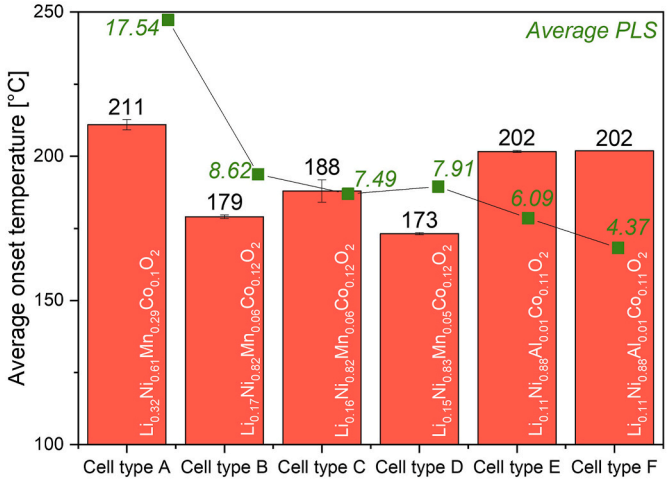

Fig. 3. The average extrapolated onset temperature together with the average penetrated layer-sets (PLS).

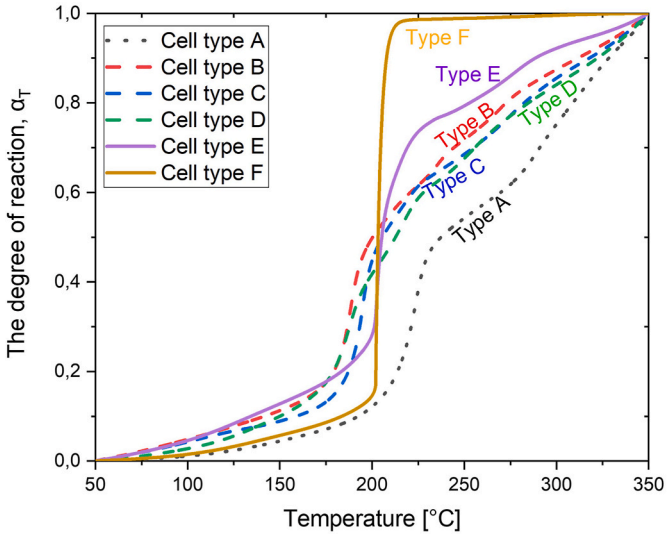

Fig. 4. The average degree of reaction vs. temperature.

tendency of LIB cells with NMC cathode active material is discussed in more details in chapter 3.3.

c. The thermal stability is dependent on Li and Ni content. When lithium content is low and nickel content is high in NMC, the reduction of Ni and Co occurs at lower temperature. Especially, highly delithiated NMC materials lose oxygen easily, which leads to a lower valence state of Ni (Ni^{2+} from Ni^{3+} and Ni^{4+}) and to transition from M_3O_4-type spinel to NiO-like rock salt structure accompanied with the oxidation reaction of electrolyte, generating thermal energy [18,19].

d. However, NCA samples from cell types E and F deviate from this trend. Even though those cathodes can be regarded as thermally stable with the second highest onset temperature, cell types E and F are the least resilient against internal short circuits. The possible explanation can be found from the observation that the reaction curves of cell E and F demonstrate the higher rate of reaction compared to other cells and those reactions occurs in a narrower temperature range (see Fig. 2). This kinetic feature is discussed in the following in Fig. 4.

e. Cell types E and F consist of the same cell chemistry and those positive electrodes hence present very similar onset temperatures, and the reaction curves are congruous.

f. In general, the reaction of NCA is much more exothermic than the NMC one, because NCA has a lower lithium content so more reactive material per unit mass, as cell type F in this work [14]. However, a non-negligible difference in exothermic reaction enthalpy between cell types E and F (approximately 400 J/g and 1100 J/g) can be found from Fig. 2 e) and f). This is because the reaction energy can vary depending on the amount of electrolyte embedded on the surface of the extracted cathode surface. It is assumed that much less electrolyte war embedded in the DSC samples of type E compared to type F.

g. Unlike cell types E and F, cell types B and C with the same positive electrode chemistry do neither present the same onset temperature nor show identical reaction curves, even though those could be categorized as a quasi-indistinguishable chemistry. It is assumed that this difference emerges from one additive to the electrolyte in cell C, namely Lithium tetrafluoro oxalate phosphate (LTFOP). This additive was found not in cell type B but only in cell type C by gas chromatography. Qin et al. and Wang et al. [20,21] have presented that LTFOP can contribute to increased safety because it helps to form solid electrolyte interface layer (SEI) and makes cathode electrolyte interface more stable. Therefore, the positive electrode with the additive LTFOP in cell type C features a higher onset temperature (188 °C) compared to the very same cathode without LTFOP in cell type B (179 °C).

The main conclusion is that thermal stability of the cathode material in the presence of electrolyte is the main contributor to the resilience of a cell against internal short circuits, more specifically, to the increased internal onset temperature to thermal runaway. In a nail penetration test, thermal runaway can be triggered when the certain amount of heat energy is generated by ISC. In respect of how the heat energy is generated and released, there is a difference between nail penetration test and DSC. An ISC induced during a nail penetration test generates thermal energy locally on the spot of the ISC in a LIB cell and the generated heat would be released rapidly over the LIB, forming a spark of heat, while a positive electrode in DSC is slowly and homogeneously heated up. The local onset temperature to TR in a nail penetration would be considerable different from the onset temperature of the positive electrode in a DSC experiment. However, if a positive electrode in a LIB cell is thermally stable, the LIB cell can endure more ISC cases or ISCs longer, which means a higher internal temperature is required for a LIB cell to initiate the reactions (mainly decomposition of cathode active materials, NMC and NCA and oxidation of electrolyte) and eventually to trigger TR. For example, a NMC cathode material with lower Ni and higher Li molar fraction starts to react at higher temperature, more specifically, it is thermally more stable. The reason is that the increased Mn^{4+} ions in a NMC sample results in suppression of the increased charge transfer resistance [5,22] but a Ni rich sample has a larger amount of unstable Ni^{4+} in its charged state, which would be easily reduced to $Ni^{3+}/^{2+}$ [19, 23]. Also, Ni molar fraction in NMC plays a crucial role to determine the onset temperature for oxygen release, because Co and Mn cation reductions occur at higher temperature. Moreover, Li^+ extraction fraction affects the structural stability [17,23].

The aluminum in $Li_{0.11}Ni_{0.88}Al_{0.01}Co_{0.11}O_2$ from cell type E and F can suppress a phase change in the crystalline structure as Mn in NMC and minimize volume change [24]. Also, the harvested NCA samples from cell type E and F react at higher onset temperature as pointed out above (listed at point d), even though cell type E and F are the least stable in the nail penetration abuse test at a cell level. To understand this contradicting behavior of NCA and a LIB cell with NCA, the degree of reaction, α_T of positive electrodes with electrolyte from cell types A to F is calculated by dividing the integrated energy until a certain temperature (T), Q_T with the total integrated ejected energy per weight from 50 to 350 °C, $Q_{50\text{-}350}$:

$$\alpha_T = \frac{Q_T}{Q_{50\text{-}350}}$$

The average degree of reaction from two DSC measurements per each sample is demonstrated in the following Fig. 4. This calculated degree of reaction in this study is limited only for the comparative study, because it is not an elementary reaction and the initial and final states of the reactions are not known [25]. In this study, a series of reactions of a positive electrode in presence of electrolyte including additives are contemplated as a whole reaction, because the study of such a whole reaction is necessary to understand commercial LIB cells and those reactions are inseparable.

In Fig. 4, the six studied automotive prismatic cell types can be categorized into three groups depending on how fast reactions proceed: the slow conversion (Cell type A) < the moderate conversion (Cell types B, C and D) < the fast conversion (Cell type E and F). The reason why cell types E and F are unstable at the cell level, even with the thermally stable NCA cathode in terms of the high onset temperature, can be found here. The NCA decomposition reaction in the presence of electrolyte is kinetically faster than for the other samples with NMC. Even though the exothermic reaction of cathode in cell types E and F is triggered later, the energy is released faster. For example, the 99 % reactions in cathode sample from cell type F and 74 % from cell type E would be carried out at 225 °C, while only 38 % (cell type A), 62 % (cell types B, C) and 59 % (cell type D) of reaction in cathode sample would be proceeded. This kinetic feature of NCA would cause heat energy to evolve faster with limited thermal diffusion or release, which induces a higher local temperature inside a cell that might eventually trigger thermal runaway. Duh et al. [26] evaluated the ranking of thermal runaway hazards of 18650 LIB cells depending on cathode materials using accelerating rate calorimeter (ARC) and observed also that the maximum self-heating rate of cells with NCA is higher than of cells with NMC and the onset temperature of an NCA cell is slightly higher than the one of an NMC cell. ARC differs from nail penetration test and DSC in respect of the adiabatic conditions in an ARC that are maintained during a Heat-Wait-Seek test [11]. Therefore, critical temperatures from ARC, DSC and nail penetration cannot be compared individually. However, the behavior of TR in a LIB cell can be compared, because the main trigger to TR in a LIB cell is thermal energy from the decomposition reaction of positive electrode in presence of electrolyte. Also, Ohneseit et al. [9] presented the corresponding results from their ARC tests; the NCA cell experiences thermal runaway earlier than NMC cells because the temperature of NCA cell increases faster than NMC cells, indicating the reaction getting faster, while the critical temperature of NMC cells is lower than NCA cells.

3.2.2. *TGA study*

Thermogravimetric analysis is used to evaluate the thermal stability by detecting mass loss in three temperature ranges as described in chapter 2.3.3. Unlike samples from cell type B and C with the same

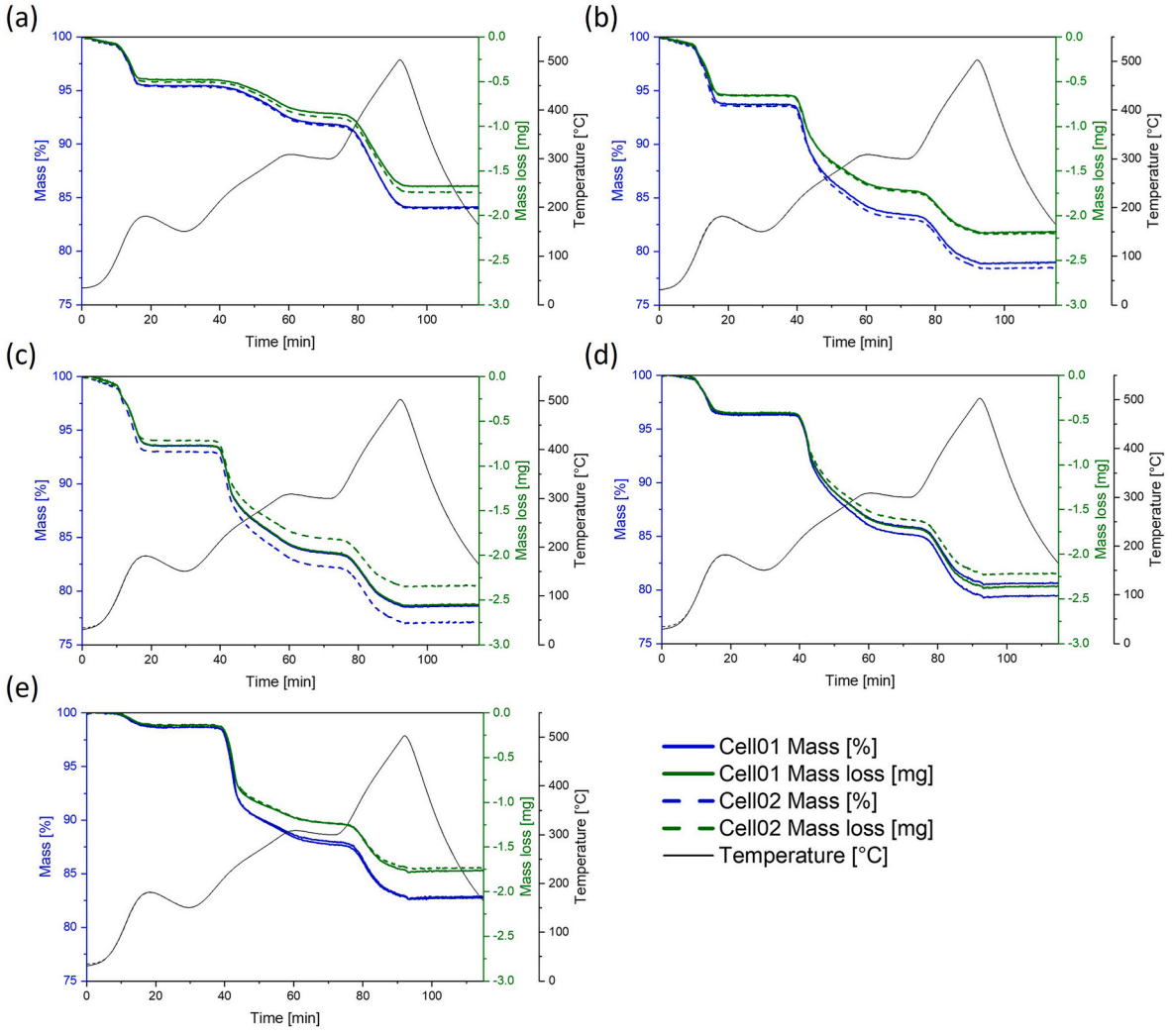

Fig. 5. TGA studies with the harvested positive electrode from 100 % SOC LIB cells: (a) Cell type A, (b) Cell type B, (c) Cell type C, (d) Cell type D and (e) Cell type F. Each sample was studied twice, and each is presented with single and dashed line.

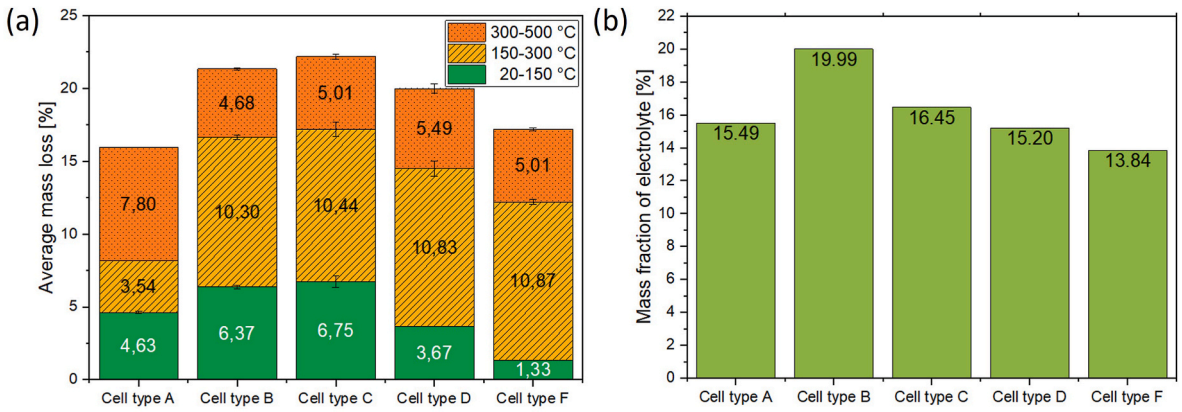

Fig. 6. The average mass loss depending on temperature range from bottom block (20–150 °C, green), middle block (150–300 °C, yellow) to top block (300–500 °C, orange) (a) and the mass fraction of electrolyte without the weight of can (b). (For interpretation of the references to colour in this figure legend, the reader is referred to the Web version of this article.)

cathode chemistry but with and without the additive LTFOP, the samples from cell type E and F present comparable results in DSC, so only a sample out of cell type F was representatively studied using TGA. To preserve the condition of cathode and its environment in a LIB cell as much as possible, the scraped off positive electrode layer was embedded in a crucible with an open lid that has a hole in the middle and the measurements were carried out under argon to minimize the exposure to ambient air possibly. The entire process from cell opening, harvesting and TGA study was conducted with a minimal time delay. The TGA result is demonstrated in Fig. 5 and the calculated average mass loss depending on three temperature ranges and mass fraction of electrolyte are presented Fig. 6. The mass fraction of electrolyte presented in Fig. 6 was determined by the subtraction of all washed and dried cell materials from the whole mass of a LIB cell.

The following observations and assumptions can be derived from Figs. 5 and 6.

a. Temperature from 20 to 150 °C with 10 K/min:

It is assumed that the electrolyte partially or entirely evaporates in this temperature range, being strongly affected by the mass fraction of electrolyte within the cells. In fact, the sample of cell type F with the smallest contribution of electrolyte to the cell mass, 13.84 % demonstrates the smallest mass loss 1.33 % in this range and most of samples lie in the same tendency; cell type F losing 1.33 % mass < cell type D with 15.20 % of electrolyte losing 3.67 % < cell type A with 15.49 % electrolyte losing 4.63 % mass. However, the sample out of cell type B with the biggest mass fraction of electrolyte loses slightly smaller mass compared to the sample out of cell type C. This is presumably because the scraped sample from cell type B would not carry the same electrolyte mass fraction, since there was a significant amount of free electrolyte without being absorbed on cell layers when cell type B was open.

b. Temperature from 150 to 300 °C with 5 K/min:

Unlike in the DSC study with the sealed crucibles, the electrolyte evaporates during TGA measurement so that it is assumed that the decomposition reaction of positive electrode would mainly take place without oxidation reaction of electrolyte. Therefore the major mass loss would result from the O_2 release [17,27,28]. From the slope of mass loss in Fig. 5, the same conclusion can be pulled out that the NCA from cell type F reacts later than other NMC samples but the reaction of NCA decomposition is faster. Also, the NMC sample with the lowest Ni - and the highest Li molar fraction demonstrate the most gradual slope in this range, since it reacts at the comparatively high temperature (Fig. 3a)) and the degree of reaction is the slowest (Fig. 4). Therefore, the NCA from cell type F loses the biggest mass fraction of 10.87 %, and NMCs out of cell types B, C and D the comparable amount from 10.30 to 10.83 %, while sample from cell type A presents the most gradual slope the smallest mass fraction loss of 3.54 %.

c. Temperature from 300 to 500 °C with 10 K/min

Presumably the residual decomposition reaction of the positive electrode would be carried out in this area. Unlike cell type B to D and F, the sample from cell type A shows the biggest mass loss above 300 °C because its reaction is kinetically limited, as seen in Fig. 4. Moreover, the total mass loss fraction of cell type A in the range from 150 to 500 °C (11.34 %) is significantly lower than other samples based on the same reason. This behavior is also observed in the work of Kasnatscheew et al. [17] presenting the decreasing mass loss of delithiated NMCs with lower Ni molar ratio in the temperature range from 180 to 370 °C.

3.3. The correlation between safety on cell level and thermal stability of the positive electrode

This comparative study aims to understand how safe automotive prismatic LIB cells are against internal short circuit and what is the key parameter to define the safety on cell level. In 3.1., several candidates as the possible key parameter are compared to the number of penetrated layer-sets (PLS) which is defined from nail penetration test as the metric to present, how resilient a LIB cell is against ISC. These were Ni-, Li-molar fraction, cell capacity, thickness of separator, thickness of current collector and mass fraction of electrolyte. A strong dependence of PLS on Ni and Li molar fraction in positive electrode is found, suggesting that the cathode active material is the main differentiator regarding cell safety. In the following chapter 3.2., the thermal stability of cathode active material is studied to understand the safety on a cell level based on the thermal stability on a material level. The Fig. 7 demonstrates that the thermal stability of the positive electrode has strong implications for battery safety on cell level. More specifically, a LIB cell with Ni-richer NMC or NCA that is thermally less stable, experiences thermal runaway with the smaller cases of ISC. This strong dependence of thermal runaway on cell level on the structural transformations of NMC or NCA accompanying the oxygen release is demonstrated also in the work of Mu et al. [29].

However, this correlation is shown only as a general inclination, since the thermal stability of positive electrode is not the only one factor but the key factor on the safety of a LIB cell. This general trend is demonstrated between three groups.

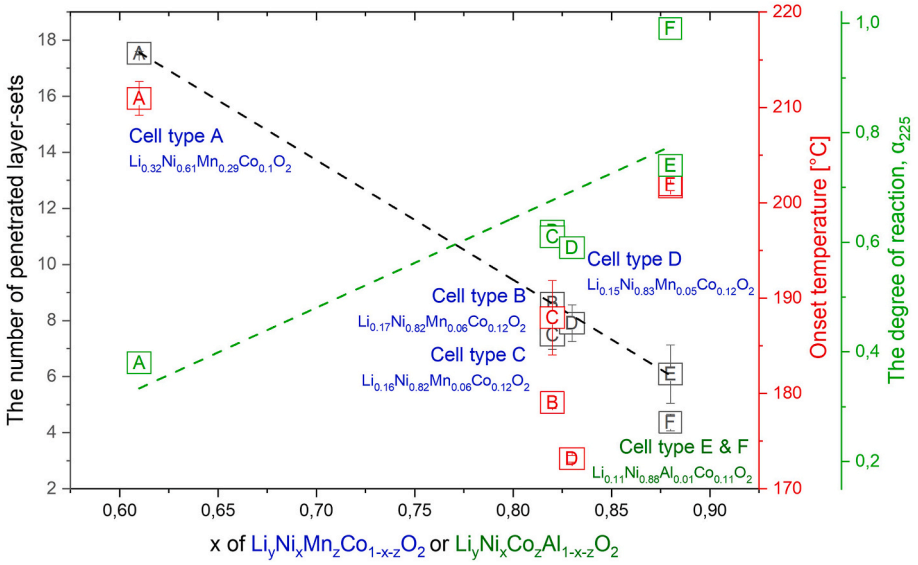

Fig. 7. The correlation between safety on cell level and thermal stability of the positive electrode.

1) The most stable cell type: cell type A consisting of NMC with significantly lower Ni fraction, 0.61 needs noticeably more ISC cases to induce thermal runaway.
2) The moderately stable cell types: cell type B, C and D with the moderate Ni molar fraction (0.82–0.83) require less PLS than cell type A but more than cell types E and F.
3) The least stable cell types: cell type E and F with NCA that has the highest Ni molar fraction (0.88) demands much less ISC cases to thermal runaway than group 1) and 2).

But within the moderately stable group, the thermal stability of positive electrode does not define the safety on cell level, since the difference in Ni- or Li molar fraction is negligible so other parameters would have a bigger impact on it, for example additives as discussed in chapter 2.3.1 (point g).

In terms of evaluating the thermal stability of positive electrode, there is one more crucial aspect besides onset temperature, namely how fast or slow reactions proceed. If only onset temperature is considered as in Fig. 3), NCA with the highest Ni molar fraction can be misevaluated as the second thermally most stable material, which contradicts the general linear trend between the battery safety and material's thermal stability. However, the decomposition reaction of NCA from cell types E and F is way faster than any other NMC samples (see Figs. 4, 5 and 7), once the onset temperature is reached.

4. Conclusions

This work begins with the question "what makes a LIB cell safer?". In this work, six automotive prismatic LIB cell types are systemically and comparatively studied using nail penetration test and the strong dependence of the critical penetration (more specifically, the number of penetrated layer-sets, PLS) on the Ni and Li molar fraction in the cathode active material is found among several possible key parameters. To understand the impact of Ni molar fraction in NMC or NCA on PLS, the positive electrodes harvested from SOC 100 % cells are studied using DSC and TGA and their thermal stability is compared in terms of extrapolated onset temperature and the degree of reaction (α_T). The main conclusions can be drawn as follows.

1. Most of automotive prismatic LIB cells consist of alike negative electrode, separator and electrolyte but different positive electrode. The battery safety on cell level depends strongly on the molar fraction of Ni and Li in the cathode active material regardless of the chemistry.
2. There is a nearly linear decrease in the thermal stability of the positive electrode in the presence of electrolyte by increasing Ni molar fraction and decreasing Li molar fraction. This thermal stability can be evaluated by two following features.
   a. Onset temperature: In the perspective of LIB cell, the onset temperature of a decomposition reaction of a positive electrode indicates the threshold temperature when a considerable amount of heat energy starts to emerge, because the cathode reaction dominates the transition to thermal runaway based on its high rate of heat release [16]. A cathode active material with lower Ni and higher Li molar fraction presents a higher onset temperature and those can be evaluated as a thermally stable material. In this study, the LIB cell's resilience against ISC with the metrics of PLS can be compared in terms of onset temperature of their NMC materials: Cell type A with biggest PLS of 17.54 (Ni = 0.61, 211 °C) > Cell types B, C and D with the metric of PLS in the range from 7.49 to 8.62 (Ni = 0.82–0.83, 173–188 °C).
   b. The degree of reaction ($\alpha_T = Q_T/Q_{50\text{-}350}$): On the cell level, a fast decomposition reaction of the cathode active material represents that thermal energy would be stacked at an accelerated rate. NCA with the highest Ni molar fraction demonstrates the significantly bigger conversion rate, even though NCA from cell types E and F starts to react at the second highest temperature. In this study, the prismatic LIB cells with NCA presents a smaller PLS compared to LIB cells with NMC: Cell types A, B, C and D with NMC showing PLS in the range from 7.49 to 17.54 > Cell types E and F with NCA presenting PLS in the range from 4.37 to 6.09.

Based on onset temperature and the degree of reaction, the thermal stability of six harvested positive electrodes with electrolyte can be listed as follow: $Li_{0.32}Ni_{0.61}Mn_{0.29}Co_{0.1}O_2$ from Cell type A (the most stable) > $Li_{0.17}Ni_{0.82}Mn_{0.06}Co_{0.12}O_2$, $Li_{0.16}Ni_{0.82}Mn_{0.06}Co_{0.12}O_2$, and $Li_{0.15}Ni_{0.83}Mn_{0.05}Co_{0.12}O_2$ from Cell types B, C and D (moderate stable) > $Li_{0.11}Ni_{0.88}Al_{0.01}Co_{0.11}O_2$ from Cell types E and F (the least stable).

3. A cathode active material with a higher thermal stability can enhance the safety of LIB on a cell level. The order of the thermal stability of the positive electrodes corresponds to the one of the safety on cell level.

4. However, the thermal stability of positive electrode is not the only parameter to define the battery safety but just the most impacting parameter on it. For example, the linear tendency between PLS and Ni or Li molar fraction can be found only in the broad framework, and cell types B and C (or cell types E and F) demonstrate slightly different robustness against ISC even with same cell chemistry. To design a safer LIB cell, the thermal stability of the positive electrode must be considered, and the composition of the cathode active material must be selectively designed, but other aspects should not be neglected.
5. On materials level, the Ni and Li molar fraction demonstrate a huge impact on thermal stability of the positive electrode with presence of electrolyte. But a small amount of additive can affect it, for example, the LTFOP in cell type C enhances the thermal stability compared to cell type B.

5. Future work

Further thermal and thermodynamic studies of DSC and TGA would be worthy with a quantified amount of electrolyte to reproduce the same mass fraction of it as in a LIB cell. In this work, the positive electrodes are studied in the presence of electrolyte (without being rinsed) possibly similar to the environment in a LIB cell. But reaction enthalpy in this comparative study cannot represent the actual thermal energy emerged from the redox reaction in a LIB cell. In case that there is large surplus of electrolyte without being adsorbed on cell layers, the result of an unrinsed positive electrode cannot represent the same mass fraction of electrolyte. For example, the mass loss fraction at low temperature area (20–150 °C) does not reflect the electrolyte mass fraction of cell type B because of the surplus (see Fig. 6) and the reaction enthalpies of samples from cell types E and F vary to a large extent even with the same chemistry (see Fig. 3b). To evaluate the contribution of the electrolyte on the thermal stability and the thermal runaway systemically, the mass fraction of the electrolyte can be accurately reproduced by applying the exact amount of it on a rinsed positive electrode. Not only the mass fraction of the electrolyte but also the influence of different electrolyte solvents can be further investigated by studying different ternary mixtures of EC, DEC, EMC and DMC.

Also, the structure of cathode active materials can be studied further, for example, if it consists of a mixture of several different materials or if it has a core-shell structure with concentration gradient. The chemical compositions defined by ICP-OES measurement represent the mean value and the further study on it has not been proceeded in this work.

Moreover, different parameters that might affect the battery safety on a cell level can be systemically analyzed. In this study, the thermal stability of the positive electrode in the presence of electrolyte is demonstrated as the key parameter but it is not the only parameter to define the battery safety. The other elements and the degree of its impact on the safety of a LIB cell can be evaluated as a next step, such as, additive, mass fraction of electrolyte and microstructure of electrodes.

CRediT authorship contribution statement

Hyojeong Kim: Writing – review & editing, Writing – original draft, Methodology, Investigation, Formal analysis, Conceptualization. **Hans Jürgen Seifert:** Writing – review & editing, Supervision. **Carlos Ziebert:** Writing – review & editing, Supervision. **Philipp Finster:** Writing – review & editing. **Jochen Friedl:** Writing – review & editing, Supervision, Project administration, Methodology, Investigation, Conceptualization.

Declaration of competing interest

The authors declare the following financial interests/personal relationships which may be considered as potential competing interests: Hyojeong Kim reports financial support was provided by BMW Group. Jochen Friedl reports financial support was provided by BMW Group. Hyojeong Kim reports a relationship with BMW Group that includes: employment. Jochen Friedl reports a relationship with BMW Group that includes: employment. If there are other authors, they declare that they have no known competing financial interests or personal relationships that could have appeared to influence the work reported in this paper.

Data availability

No data was used for the research described in the article.

Acknowledgments

Bayerische Motoren Werke AG is gratefully acknowledged for their financial support. We want to thank Julia Endres for the ICP-OES measurement. This research was partly funded by the Helmholtz Association, in the programme Materials and Technologies for the Energy Transition (MTET), grant number FE.5341.0118.0012, and we want to express our gratitude for the funding. It contributes to the research performed at CELEST (Center of Electrochemical Energy Storage Ulm-Karlsruhe).

References

[1] Y. Xia, J. Zheng, C. Wang, M. Gu, Nano Energy 49 (2018) 434–452, https://doi.org/10.1016/j.nanoen.2018.04.062.
[2] M. Brand, S. Glaser, J. Geder, S. Menacher, S. Obpacher, A. Jossen, D. Quinger, in: 2013 World Electric Vehicle Symposium and Exhibition (EVS27), IEEE, 112013, pp. 1–9..
[3] J. Chen, L. Zhu, Di Jia, X. Jiang, Y. Wu, Q. Hao, X. Xia, Y. Ouyang, L. Peng, W. Tang, T. Liu, Electrochim. Acta 312 (2019) 179–187, https://doi.org/10.1016/j.electacta.2019.04.153.
[4] A. Kvasha, C. Gutiérrez, U. Osa, I. de Meatza, J.A. Blazquez, H. Macicior, I. Urdampilleta, Energy 159 (2018) 547–557, https://doi.org/10.1016/j.energy.2018.06.173.
[5] H.-J. Noh, S. Youn, C.S. Yoon, Y.-K. Sun, J. Power Sources 233 (2013) 121–130, https://doi.org/10.1016/j.jpowsour.2013.01.063.
[6] Y. Huang, Y.-C. Lin, D.M. Jenkins, N.A. Chernova, Y. Chung, B. Radhakrishnan, I.-H. Chu, J. Fang, Q. Wang, F. Omenya, S.P. Ong, M.S. Whittingham, ACS Appl. Mater. Interfaces 8 (2016) 7013–7021, https://doi.org/10.1021/acsami.5b12081.
[7] J. Zheng, T. Liu, Z. Hu, Y. Wei, X. Song, Y. Ren, W. Wang, M. Rao, Y. Lin, Z. Chen, J. Lu, C. Wang, K. Amine, F. Pan, J. Am. Chem. Soc. 138 (2016) 13326–13334, https://doi.org/10.1021/jacs.6b07771.
[8] S. Hwang, S.M. Kim, S.-M. Bak, B.-W. Cho, K.Y. Chung, J.Y. Lee, W. Chang, E. A. Stach, ACS Appl. Mater. Interfaces 6 (2014) 15140–15147, https://doi.org/10.1021/am503278f.
[9] S. Ohneseit, P. Finster, C. Floras, N. Lubenau, N. Uhlmann, H.J. Seifert, C. Ziebert, Batteries 9 (2023) 237, https://doi.org/10.3390/batteries9050237.
[10] D.H. Doughty, E.P. Roth, Electrochem. Soc. Interface 21 (2012) 37.
[11] H. Kim, A. Sahebzadeh, H.J. Seifert, C. Ziebert, J. Friedl, J. Power Sources 592 (2024) 233902, https://doi.org/10.1016/j.jpowsour.2023.233902.
[12] X. Feng, M. Quyang, X. Liu, L. Lu, Y. Xia, X. He, Energy Storage Mater. 10 (2018) 246, https://doi.org/10.1016/j.ensm.2017.05.013.
[13] J. Lamb, C.J. Orendorff, E.P. Roth, J. Langendorf, J. Electrochem. Soc. 162 (2015) A2131.
[14] R.C. Shurtz, J. Electrochem. Soc. 167 (2020) 140544, https://doi.org/10.1149/1945-7111/abc7b4.
[15] R.C. Shurtz, J.D. Engerer, J.C. Hewson, J. Electrochem. Soc. 165 (2018) A3878–A3890, https://doi.org/10.1149/2.0541816jes.
[16] R.C. Shurtz, J.C. Hewson, J. Electrochem. Soc. 167 (2020) 90543, https://doi.org/10.1149/1945-7111/ab8fd9.
[17] J. Kasnatscheew, S. Röser, M. Börner, M. Winter, ACS Appl. Energy Mater. 2 (2019) 7733–7737, https://doi.org/10.1021/acsaem.9b01440.
[18] C. Tian, Y. Xu, W.H. Kan, D. Sokaras, D. Nordlund, H. Shen, K. Chen, Y. Liu, M. Doeff, ACS Appl. Mater. Interfaces 12 (2020) 11643–11656, https://doi.org/10.1021/acsami.9b21288.
[19] S.-M. Bak, E. Hu, Y. Zhou, X. Yu, S.D. Senanayake, S.-J. Cho, K.-B. Kim, K.Y. Chung, X.-Q. Yang, K.-W. Nam, ACS Appl. Mater. Interfaces 6 (2014) 22594–22601, https://doi.org/10.1021/am506712c.
[20] Y. Qin, Z. Chen, J. Liu, K. Amine, Electrochem. Solid State Lett. 13 (2010) A11, https://doi.org/10.1149/1.3261738.
[21] J. Wang, D. Zhao, Y. Cong, N. Zhang, P. Wang, X. Fu, X. Cui, ACS Appl. Mater. Interfaces 13 (2021) 16939–16951, https://doi.org/10.1021/acsami.0c21535.
[22] W. Li, S. Lee, A. Manthiram, Advanced materials (Deerfield Beach, Fla.) 32 (2020) e2002718, https://doi.org/10.1002/adma.202002718.
[23] S. Hwang, S.M. Kim, S.-M. Bak, S.Y. Kim, B.-W. Cho, K.Y. Chung, J.Y. Lee, E. A. Stach, W. Chang, Chem. Mater. 27 (2015) 3927–3935, https://doi.org/10.1021/acs.chemmater.5b00709.

[24] G. Mulder, N. Omar, S. Pauwels, M. Meeus, F. Leemans, B. Verbrugge, W. de Nijs, P. van den Bossche, D. Six, J. van Mierlo, Electrochim. Acta 87 (2013) 473–488, https://doi.org/10.1016/j.electacta.2012.09.042.
[25] Dr.G.W. H. Höhne, Dr.W.F. Hemminger, Dr.H.-J. Flammersheim, Differential Scanning Calorimetry, 2nd, Springer, Berlin Heidelberg, 2003.
[26] Y.S. Duh, Y. Sun, X. Lin, J. Zheng, M. Wang, Y. Wang, X. Lin, X. Jiang, Z. Zheng, S. Zheng, G. Yu, J. Energy Storage 41 (2021) 102888, https://doi.org/10.1016/j.est.2021.102888.
[27] D.J. Xiong, L.D. Ellis, J. Li, H. Li, T. Hynes, J.P. Allen, J. Xia, D.S. Hall, I.G. Hill, J. R. Dahn, J. Electrochem. Soc. 164 (2017) A3025–A3037, https://doi.org/10.1149/2.0291713jes.
[28] J. Lamb, L. Torres-Castro, J.C. Hewson, R.C. Shurtz, Y. Preger, J. Electrochem. Soc. 168 (2021) 60516, https://doi.org/10.1149/1945-7111/ac0699.
[29] L. Mu, Q. Yuan, C. Tian, C. Wei, K. Zhang, J. Liu, P. Pianetta, M.M. Doeff, Y. Liu, F. Lin, Nat. Commun. 9 (2018) 2810, https://doi.org/10.1038/s41467-018-05172-x.